https://ntrs.nasa.gov/search.jsp?R=19890017841 2020-03-20T01:57:41+00:00Z

NASA Technical Memorandum 101580

# STRUCTURAL ANALYSIS OF A THERMAL INSULATION RETAINER ASSEMBLY

William H. Greene and Carl E. Gray, Jr.

July 1989

(NASA-TM-101580) STRUCTURAL ANALYSIS OF A THERMAL INSULATION RETAINER ASSEMBLY (NASA. Langley Research Center) 27 p CSCL 20K

N89-27212

Unclas
G3/39 0224102

National Aeronautics and Space Administration

Langley Research Center
Hampton, Virginia 23665

# STRUCTURAL ANALYSIS OF A THERMAL INSULATION RETAINER ASSEMBLY

William H. Greene and Carl E. Gray, Jr.
Langley Research Center

## Introduction

In January 1989 an accident occurred in the National Transonic Facility wind tunnel at NASA Langley Research Center. It is believed that the failure of a insulation retainer, the thermal barrier clamp assembly (TBCA) shown in figure 1, holding foam insulation around the fan drive shaft resulted in the subsequent damage to other components in the tunnel.

This insulation-retainer-assembly consists of two roughly semicircular stainless steel bands (figure 2) which are placed around the insulation on the shaft and then connected together with the two clamp assemblies at 0 and 180 degrees. Each clamp assembly includes four stiff stainless steel bars (figure 3). Two bars are attached with screws to the fore and aft ends of each stainless steel band. Then seven bolts are used between the bars at each clamp assembly to clamp the bands together.

Two loading cases are particularly significant for the insulation band assembly. The first case is a centrifugal force due to the rotation of the shaft. The mass of the insulation and the mass of the band itself create a uniform outward radial load on the band. The mass of the clamp bars applies a large outward radial load at the 0 and 180 degree locations. The second loading case occurs when the tunnel is operating under cryogenic conditions. In this case the band is colder than the shaft which is thermally isolated by the insulation. Under this condition the retainer-band tries to shrink inward but is restrained from doing so by the elastic interface of the insulation and the relatively stiff interface of the shaft below.

The objective of this report is to describe the structural behavior of the retainer-band under the typical loading conditions mentioned above. The stresses in the region

of the clamp assembly are of particular interest in understanding the failure of the part. Finite element analyses using several models and loading conditions have been performed to understand the structural response. The basic approach used in the analysis, the finite element models, and the most significant results from the analyses are discussed below.

## Retainer-Band Design

The retainer-band described above is designed to keep blocks of foam thermal insulation in contact with the fan shaft. The fan shaft has a diameter of 48 inches and the insulation blocks have a thickness of two inches. The insulation was assumed to have $E = 10000.$ psi, $\nu = 0.3$, and $\rho = 0.0088$ lbs/in$^3$ where $E$, $\nu$, and $\rho$ are the Young's modulus, Poisson's ratio, and density of the material respectively.

The diameter of the band is 52 inches and its length along the shaft is 24.88 inches. Each half of the band is constructed of 0.035 inch stainless steel sheet. The properties assumed for this material are $E = 28 \times 10^6$ psi, $\nu = 0.3$, $\rho = 0.283$ lbs/in$^3$, $\alpha = 9.6 \times 10^{-6}$ in/in/°F, $\sigma_y = 35$ ksi, and $\sigma_u = 85$ ksi where $\alpha$ is the coefficient of thermal expansion, $\sigma_y$ is the allowable yield stress for the material, and $\sigma_u$ is the allowable ultimate stress for the material.

There are four clamp blocks making up each of the two joints(fig. 3). The two "short" blocks in each clamp assembly are 6.38 inches long, approximately 1.0 inches wide, approximately 2.2 inches high and constructed from stainless steel. The two "long" blocks in each clamp assembly are 13.0 inches long and have the same cross sectional dimensions and material as the short blocks. The two short blocks are connected across the clamp assembly by 3 bolts and the two long blocks are connected by 4 bolts as shown in figure 3. Each of these bolts includes a stack of Belleville washers to allow expansion of the band. In the analysis each stack of Belleville washers was assumed to have a linear spring stiffness until they bottom out at a force of 1200 lbs and a compression of 0.077 inches. There is considerable doubt that the Belleville washers were effective in actual practice. Under the centrifugal loading it is quite possible that deflections in the clamp assembly prevented the sliding between the clamp bars required to load the Belleville washers. Results for

cases with the Belleville washers working and not working are considered below. A cross-sectional view of an assembled joint is shown in figure 4. The total mass of a clamp assembly was taken as 25.3 lbs in the analysis.

An aluminum ring, which is not strictly part of the retainer-band design, is also attached to the clamp assembly. The ring has a height of 1.96 inches, an average thickness of 0.41 inches and encircles the band and drive shaft. The 6061-T651 aluminum material has an $E = 10 \times 10^6$ psi, $\rho = 0.1$ lbs/in$^3$, an $\alpha = 14 \times 10^{-6}$ in/in/°F, $\sigma_y = 35$ ksi, and a $\sigma_u = 42$ ksi. The ring is attached to the band assembly with screws at the inboard (between the long and short blocks) end of the short blocks. In order to allow the ring to be placed around the shaft, the ring contains joints at the 0 and 180 degree locations. However, the joints were broken by normal, operational loads sometime during the six-year operation of the tunnel. The effect on the band assembly of this ring with and without the functional joints will be considered in the analysis section.

## Analytical Approach

As the retainer-band deforms under the centrifugal loading, it tries to assume an oval shape. This occurs because the concentrated mass at the clamp bars causes large radially outward inertia loads at these locations. The band is constrained from moving inward, however, by the insulation and the shaft but is free to move radially outward. Under the centrifugal loading various regions of the band will be compressed against the insulation while other regions will have pulled away. Accounting for this variable contact region significantly complicates the analysis.

Another complication in the analysis is concerned with the mechanism by which the band carries this non-uniform centrifugal load. Because the band is thin its resistance to the transverse centrifugal load only occurs **after** it has rotated radially outward. That is, the stiffness of the band in the transverse direction, in its undeformed shape is essentially zero.

Accurately representing the stiffness of the band and accounting for the changing contact region under load requires a nonlinear finite element analysis. Accordingly, the

geometric nonlinear analysis capability of EAL (ref. 1) was used. EAL handles the deflection dependent stiffening of the band directly. However, modifications to the geometric nonlinear analysis procedures were required to handle the variable contact. A modification was made to allow the direct inclusion of a nonlinear (piecewise linear) relation between any two degrees of freedom in the model. For example, contact is modeled by specifying a force displacement curve with high compression stiffness and near zero tensile stiffness between the two degrees of freedom normal to the contacting surfaces. In the finite element models these piecewise linear relations were specified between all points where contact could potentially occur. During the solution of the nonlinear equations, the status of each contact point is directly determined. This directly-specified-nonlinear-relation approach also allowed the straightforward modeling of the Belleville washers when their effect was considered in the analysis.

The nonlinear solution process for the retainer assembly is not only computationally costly but is also numerically difficult. The numerical difficulties occur because the band is thin, transversely loaded with concentrated edge load (clamp block mass), and attached to a much stiffer component (clamp blocks). Because the band is thin its bending stiffness is low. The resistance to the transverse load occurs only after it deflects. This makes the response highly nonlinear. Even with small increments in loading, the solution process often has convergence difficulties. For this reason, results for some geometry/loading cases, that would otherwise be of interest, are not included in this report.

## Finite Element Models

A number of different finite element models were developed to study the structural behavior of the retainer-band. Four of these models will be described here. All four models consider only a 90 degree segment of the band with symmetry conditions applied at 0 and 90 degrees. The primary difference between Models 1 and 2 is that Model 1 includes elastic solid finite elements to model the insulation while Model 2 does not. Including these elements doubles the size of the model, complicates the solution process, and significantly increases the computational time required for solution when the centrifugal load is applied. Because of the large computational times required for a nonlinear solution to the centrifugal

load case, a third, much simpler model was developed. Model 3 is a 2-D model which contains only a single row of elements along the length of the shaft but does include the elastic solid elements to model the insulation. Model 4 is also a 2-D model that was developed to get a better estimate of the bending stresses in the band near the clamp bars. Results from all four models are presented in the analytical results section.

Although Model 1 includes the insulation, the elements representing the insulation are not shown in figure 5. Model 2, which does not include the insulation, is shown in figure 6. Although Model 2 does not include the insulation, it does contain several improvements relative to Model 1. As seen in figure 6, the clamp bar region in Model 2 is more refined. The clamp bar itself is modeled with plate elements instead of the beam elements in Model 1 and the finite element mesh in the band is denser near the clamp bar. In both models beam elements representing the seven bolts extend from the appropriate location at the clamp bar to the symmetry plane at $\theta = 90°$. The refinement of the clamp bar in Model 2 allowed the optional inclusion of the Belleville washers. These are modeled by specifying the appropriate nonlinear force-displacement relation between the bolt circumferential displacements and the symmetry plane at $\theta = 90°$. In Model 1 contact is considered between each radial degree of freedom in the band and the corresponding radial degree of freedom in the insulation. In Model 2 contact is considered between the band degrees of freedom and ground. Uniform nonstructural mass is added to the band shell elements in both models to represent the centrifugal loading effect of the insulation. In both models it is possible to optionally include the aluminum ring. In Model 2 the ring is modeled with plate elements and is clearly shown in figure 6. In Model 1 the ring is modeled with beam elements and is shown as the darkened line in figure 5.

Model 3 consists of a single row of plate elements representing the band with a single row of elastic solid elements representing the insulation from $\theta = 0°$ to $\theta = 90°$. In Model 3, the representation of the clamp bar region is very simplified. The stiffness and mass effects due to the clamp assembly are assumed to all occur at the $\theta = 90°$ symmetry plane.

A detailed view of the clamp assembly is shown in figure 4. In this figure it can be seen that the stainless steel band wraps around the clamp bar with a $90°$ bend and is fastened to the clamp bars with a support bar and cap screws. When the clamp bar moves

radially outward under the centrifugal loading, the stainless steel band bends away from the clamp bar. To obtain a better estimate of the bending stresses in the band where it contacts the clamp bar, Model 4 was developed and is shown in figure 7. This is a 2-D model where beam elements were used to represent the band and plane stress elements were used to represent the clamp bar. A beam element was also used to give a smeared, plane stress representation of the bolts attaching the clamp bar to the $\theta = 90°$symmetry plane.

## Analytical Results

The structural response of the retainer assembly was evaluated for two load cases using the finite element models described in the previous section. The load cases considered were the mechanical loads due to the fan shaft rotating at 580 rpm and a thermal loading of $-100°F$ temperature difference between the components of the retainer assembly and the fan shaft. A summary of of results for these two loading conditions applied to various retainer assembly configurations is shown in table 1.

### Centrifugal Load Cases

The baseline analysis case consists of Model 2 without the aluminum ring and without the effect of the Belleville washers. The resulting deflection pattern is shown in the contour plot of figure 8 and the deformed geometry plot of figure 9. Figure 8 shows that the band has lifted away from the shaft over a significant region near $\theta = 90°$. The maximum deflection occurs at the clamp bar and is 0.28 inches. A contour plot of the effective stress at the midsurface of the band is shown in figure 10. The maximum stresses occur near the ends of the clamp bars. The values of $\sigma_\theta$ near the outboard end of the long bar, the inboard end of the long bar, the inboard end of the short bar, and the outboard end of the short bar are 35 ksi, 41 ksi, 32 ksi, and 33 ksi respectively. The nominal stress away from the clamp bars is approximately 22 ksi.

Model 2 does not include the effect of the insulation. In order to estimate the effect of the insulation on deflections and stresses the 2-D model, Model 3, was analyzed under the centrifugal loading case. The maximum deflection with the insulation modeled is 0.36

inches and without the insulation is 0.32 inches. In this model the stress concentrations around the clamp bar ends do not occur and the stress from both the case with insulation and without insulation is about 24 ksi. Based on these results, we believe that not including the insulation in the model has only a small effect on the results from the centrifugal load case.

Another case considered the effect of including the ring with the unbroken joint but assuming that the Belleville washers are ineffective. A contour plot of effective stress is shown in figure 11. The ring is picking up a portion of the load previously carried by the skin. However, because the inboard end of the short clamp bar is held by the ring a very large stress (80 ksi) is developed near the outboard end of the short bar. The effective stress in the ring is relatively low, however, as shown in figure 12. Clearly the lack of movement in the joint without the Belleville washers contributes to keeping the ring stress low. The stresses for the case with the broken ring are similar to the case with the unbroken ring as shown in figure 13. Again, there is a large stress (75 ksi) near the outboard end of the short bar.

A case with the Belleville washers effective but without the ring was also considered. The radial deflection a the clamp bar has increased to approximately 0.57 inches. The deflection pattern is shown in the deformed geometry plot of figure 14. The maximum values of $\sigma_\theta$ occur near the ends of the clamp bars and are slightly reduced from the case without the Belleville washers. The effective stress is shown in the contour plot of figure 15. The values of $\sigma_\theta$ near the outboard end of the long bar, the inboard end of the long bar, the inboard end of the short bar, and the outboard end of the short bar are 29 ksi, 34 ksi, 27 ksi, and 29 ksi respectively.

From the results of Models 1 and 2 and from intuition is was clear that bending stresses in the band near the clamp bars were high. It was also clear that these stresses were strongly influenced by the detailed geometry and contact pattern between the band and clamp bar. To estimate these stresses the centrifugal loading was applied to Model 4. The maximum displacement for this model is approximately 0.4 inches compared with 0.28 inches for Model 2 and 0.32 inches for Model 3. This larger deflection is likely due to the more refined modeling of the band – clamp bar interface. As can be seen in figure 7,

the band is pulling away from the clamp bar radius. In this region, the band initially has a radius of curvature equal to the clamp bar radius but is nearly flattened under the loading. The result of this large curvature change is high bending stress in this area of the band; outer fiber bending stresses range from 120 ksi to 194 ksi. Obviously these high stresses predicted by an elastic analysis are not present in the actual structure. They do indicate, however, that repeated yielding in this region is likely under the repeated application of the centrifugal loads.

### Thermal Load Cases

The thermal load considered was a $\Delta T = -100\,^{\circ}F$ between the retainer-band and the shaft. The temperature of the insulation was assumed to be equal that of the shaft. The baseline analysis case for this loading consists of Model 1 without the aluminum ring and without the effect of the Belleville washers. The deformation pattern is nearly uniform inward motion of the band. Because the Belleville washers are assumed not to be present, the stresses are high as can be seen in the contour plot of effective stress in figure 16. As in the centrifugal loading case, the maximum stresses occur near the ends of the clamp bars. The values of $\sigma_\theta$ near the outboard end of the long bar, the inboard end of the long bar, the inboard end of the short bar, and the outboard end of the short bar are 26 ksi, 36 ksi, 36 ksi, and 24 ksi respectively.

When Model 2, which does not include the insulation, is used for this loading condition the maximum $\sigma_\theta$ is approximately 49 ksi. This is 36% higher than the result from Model 1. Clearly, it is important to include the effect of the insulation in considering the thermal loads.

Model 2 was used, however, to consider the effect of the thermal load when the Belleville washers are included in the model. In this case, the maximum $\sigma_\theta$ is quite low (9 ksi) indicating that if the Belleville washers are effective, the thermal loading is not significant.

The effect of the aluminum ring on the band in the presence of the thermal load was considered using Model 1. Two cases were analyzed. In the first case the joints in the ring are assumed to be intact and in the second case the joints are assumed to have failed. This

effect is modeled by either constraining the appropriate degrees of freedom on the ring nodes at the 90° symmetry plane or releasing them. In both cases, the Belleville washers are assumed not to be effective. When the ring is intact, the values of $\sigma_\theta$ near the outboard end of the long bar, the inboard end of the long bar, the inboard end of the short bar, and the outboard end of the short bar are 27 ksi, 33 ksi, 59 ksi, and 22 ksi respectively. The effective stress for this case is shown in the contour plot of figure 17. The maximum stress in the ring for this case is only about 5 ksi. When the ring is broken, the values of $\sigma_\theta$ near the ends of the clamp bars are the same as when the ring is assumed to be missing. The maximum stress in the ring is less than one ksi. These results are significantly affected by the assumption that the Belleville washers are not present.

To bound the value of maximum ring stress under the thermal load, cases were considered with Model 2 and with the Belleville washers present. In these cases the skin is allowed considerable freedom to shrink except in the vicinity of the ring. The first case assumes that the ring is not broken at the joint. The result as shown in the contour plot of effective stress in figure 18 is a very high stress in the skin near the ring. The maximum stresses in the ring are also high. A contour plot of effective stress in the ring is shown in figure 19. The maximum stress of 28 ksi is near the 35 ksi yield stress for the aluminum. The second case assumes that the ring joint has broken. The stresses for this case are highest in the skin but considerably lower than for the case with the unbroken ring. The effective stress in the skin is shown in the contour plot of figure 20. The stresses in the ring, as shown in figure 21, are also much lower than for the case with the unbroken ring. When the Belleville washers are working, the stresses due to the thermal loading are low except for the case when the ring joint is still intact.

## Concluding Remarks

A nonlinear finite element analysis of an insulation-retainer-assembly has been completed. A nonlinear analysis was required to model both the stress-stiffening in the thin band and the variable contact regions between components. Two loading conditions, a centrifugal load due to the rotating shaft and a thermal load due to cooling of the retainer-assembly relative to the shaft, were considered. Cases with and without an attached

aluminum ring and with and without a Belleville washer stress relief mechanism were considered.

The purpose of the Belleville washers is to reduce the stresses under the thermal loading. Analyses confirmed that if the Belleville washers were present in the model the stresses were low except for the case with the unbroken aluminum ring. In this case high stresses are developed in the skin near the ring and at the end of the ring itself. Considering the reduced area in the ring due to the fastener holes and stress concentrations around the fasteners, it is likely that this loading condition would break the ring at the joint.

Thermal analyses without the Belleville washers working showed stress concentrations in the band near the inboard ends of the two clamp bars. These stresses could have contributed to failure especially if combined with those from the centrifugal load case.

Under the centrifugal load, high, local, membrane stresses also occur in the skin near the ends of the clamp bars. The presence of the Belleville washers has little effect on the stresses for this case. The addition of either the unbroken or broken aluminum ring, however, causes a large local stress (70 ksi) to be developed in the band near the outboard end of the short block. Analyses with the 3-D models under the centrifugal load suggest that high bending stresses are being developed where the band contacts the clamp blocks.

To estimate these bending stresses, a 2-D model was developed with considerable detail in the area of the band – skin contact. This model predicted bending stresses on the order of 200 ksi. Since this stress is beyond the ultimate stress of the material, significant yielding must be taking place in this region. Based on the analyses conducted to date, we believe these high bending stresses are the most likely contributor to the failure of the part.

# Reference

1. Whetstone, W. D., *EISI-EAL Engineering Analysis Language Reference Manual – EISI-EAL System Level 312.* Engineering Information Systems, Inc., August 1985.

# TABLE 1 - FINITE-ELEMENT CASE SUMMARY

| GEOMETRY\LOADING | MECHANICAL (580 RPM) | THERMAL (-100 F) |
|---|---|---|
| BELV. NOT WORKING<br>RING OFF | 2-08 DISPLACEMENT CONTOURS<br>2-09 DEFORMED GEOMETRY<br>2-10 VON MISES STRESS BAND | 1-16 VON MISES STRESS |
| BELV. NOT WORKING<br>RING ON | 2-11 VON MISES STRESS BAND<br>2-12 VON MISES STRESS RING | 1-17 VON MISES STRESS |
| BELV. NOT WORKING<br>RING BROKEN | 2-13 VON MISES STRESS BAND | RESULTS SIMILAR TO 1-16 |
| BELV. WORKING<br>RING OFF | 2-14 DEFORMED GEOMETRY<br>2-15 VON MISES STRESS BAND | ( STRESS < ~6 KSI) |
| BELV. WORKING<br>RING ON | NA | 2-18 VON MISES STRESS BAND<br>2-19 VON MISES STRESS RING |
| BELV. WORKING<br>RING BROKE | NA | 2-20 VON MISES STRESS BAND<br>2-21 VON MISES STRESS RING |
| DETAILED BAND RADIUS<br>CONTACT MODEL | BENDING STRESS = 200 KSI | NA |

key: x-yy 'x'='analysis model'; 'yy'='figure number displaying results'

ORIGINAL PAGE
COLOR PHOTOGRAPH

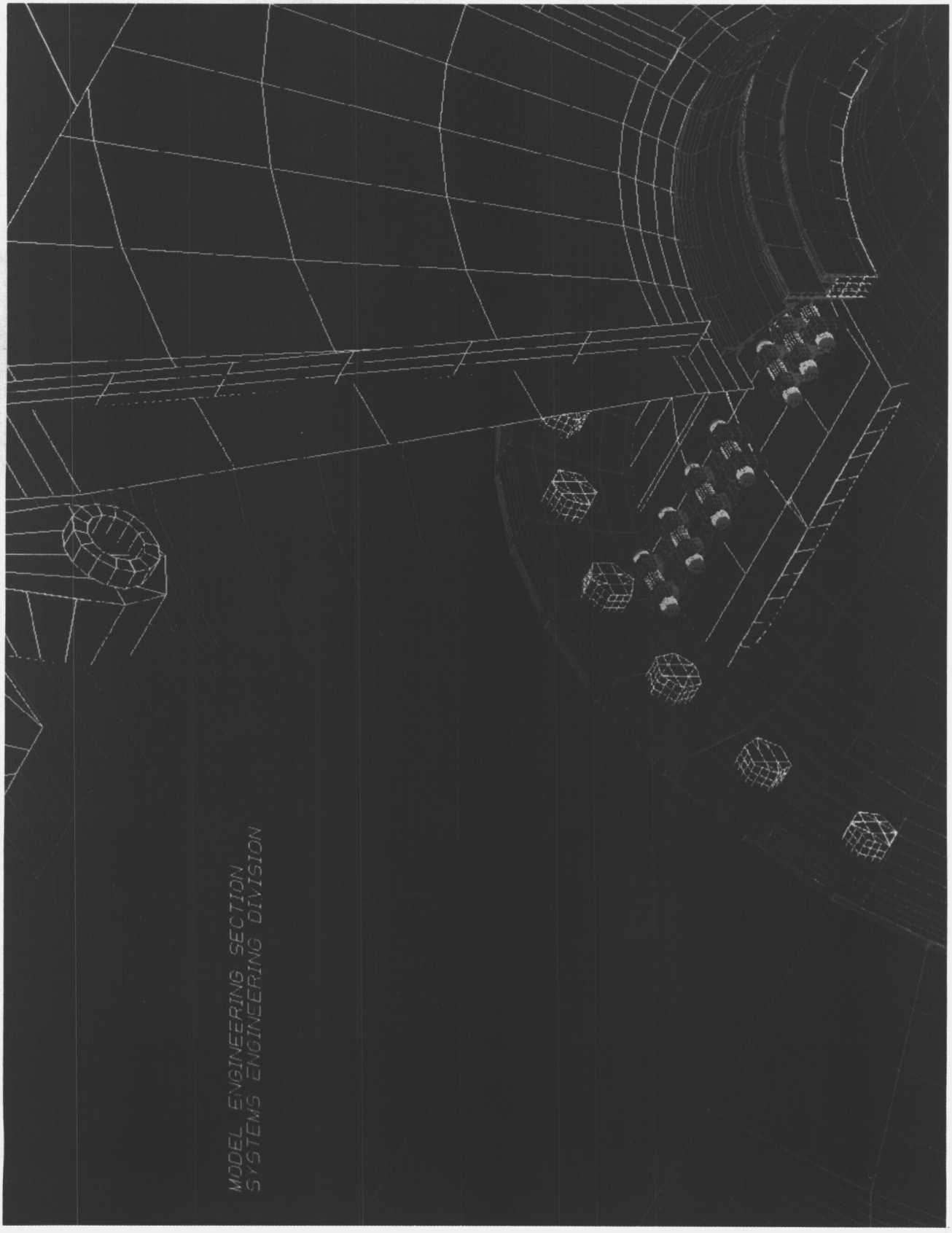


Figure 1.- NTF fanshaft external thermal barrier clamp assembly installed on the shaft.

Figure 2.- Insulation retainer band.



ORIGINAL PAGE
BLACK AND WHITE PHOTOGRAPH

ORIGINAL PAGE
COLOR PHOTOGRAPH

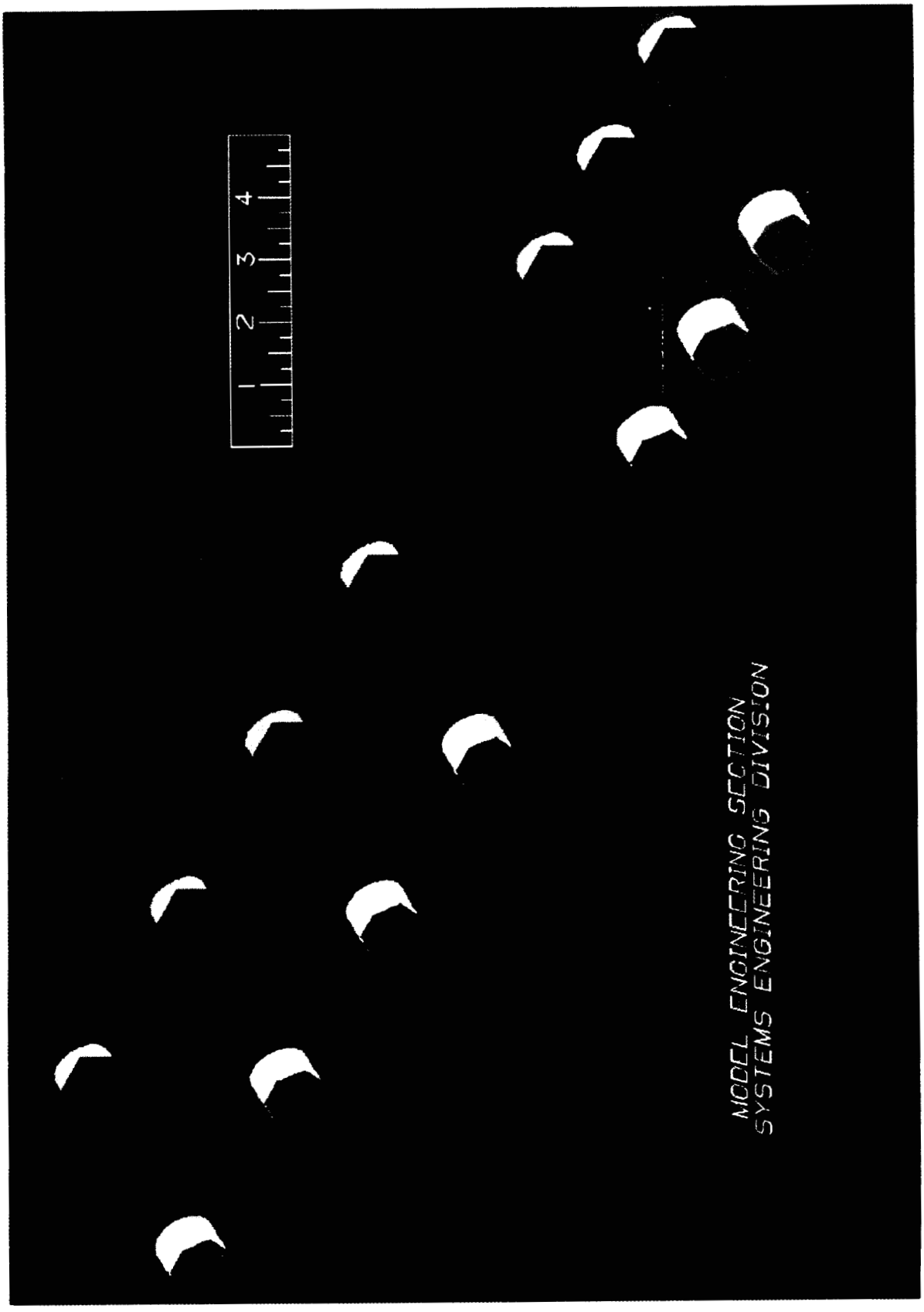


Figure 3.- "Long" and "short" block components of the insulation retainer assembly.

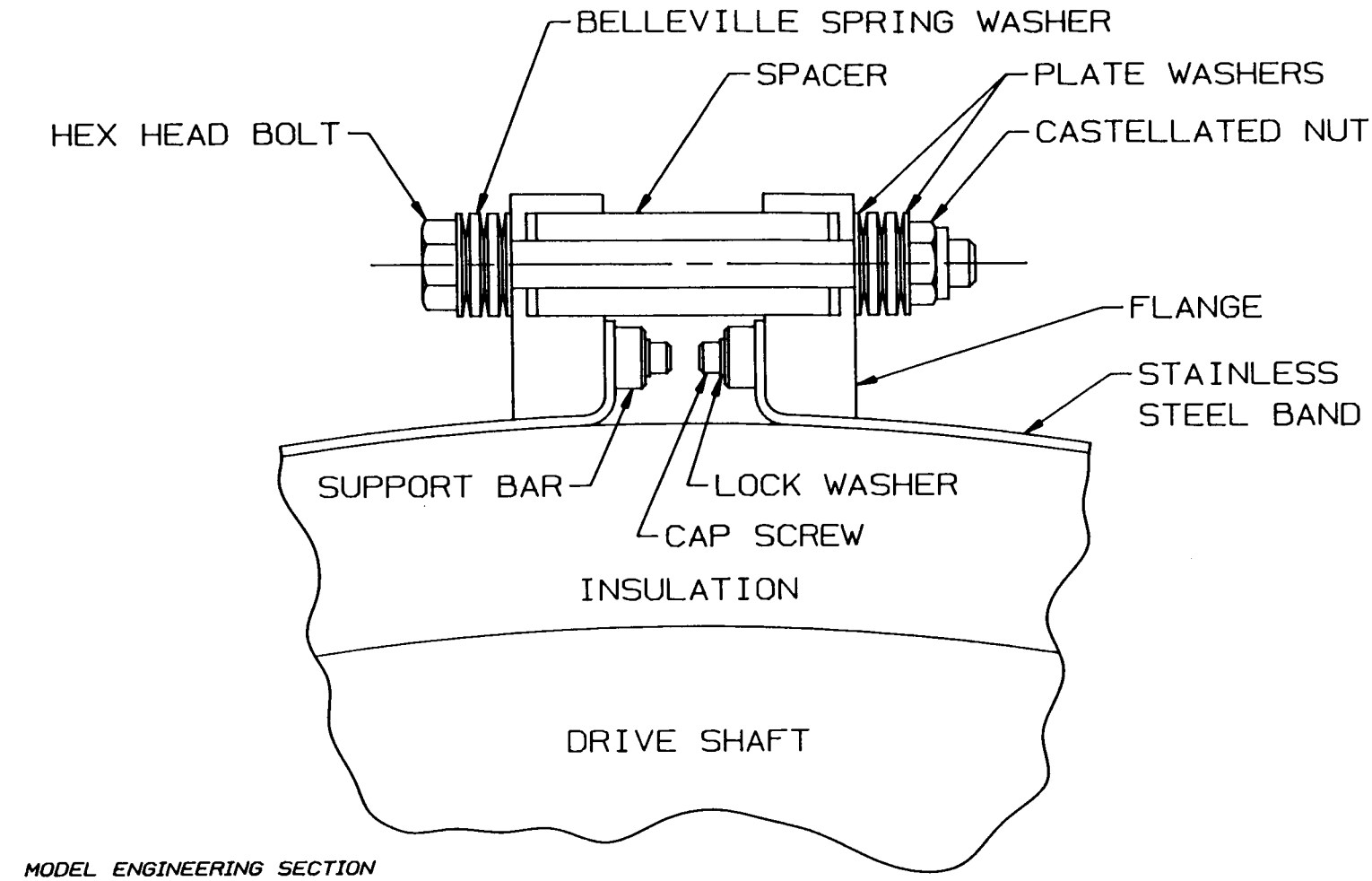


Figure 4.- Cross sectional view of the clamp region of the insulation retainer assembly.

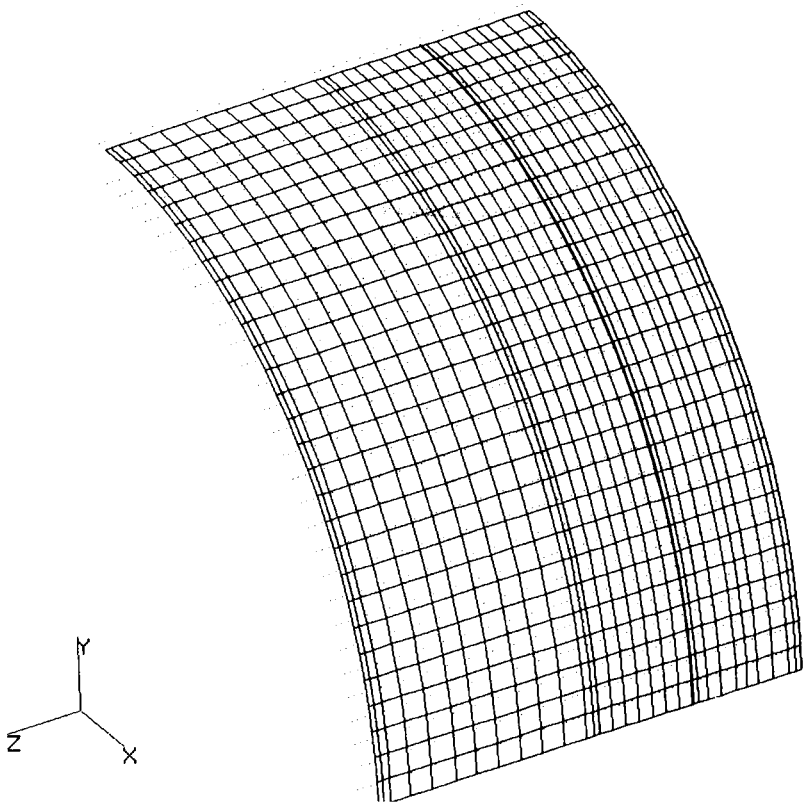


Figure 5.- Finite element model (Model 1) of insulation retainer assembly including insulation.

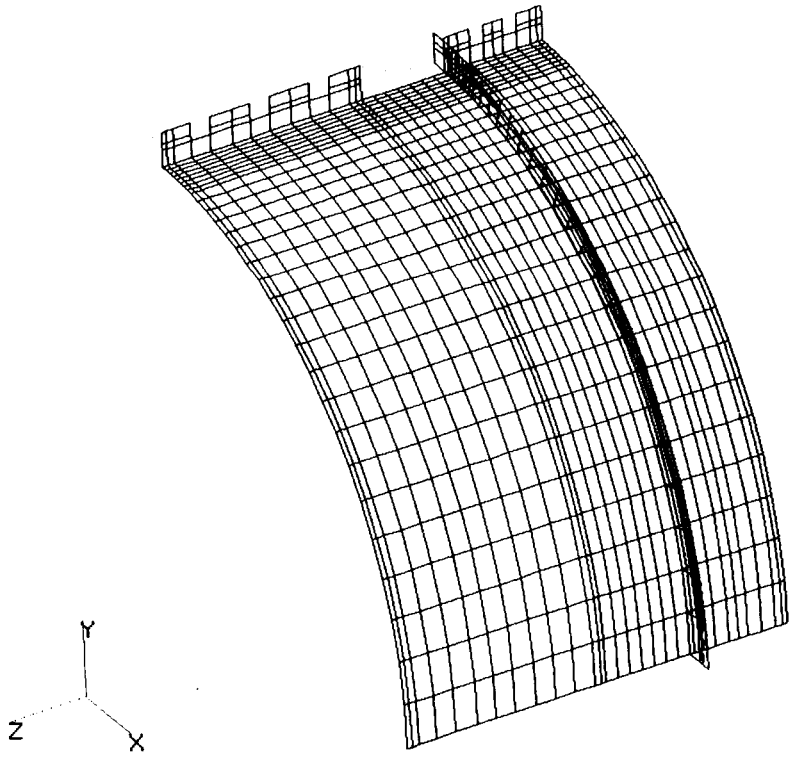


Figure 6.- Finite element model (Model 2) of insulation retainer assembly with a refined clamp-bar region but without insulation.

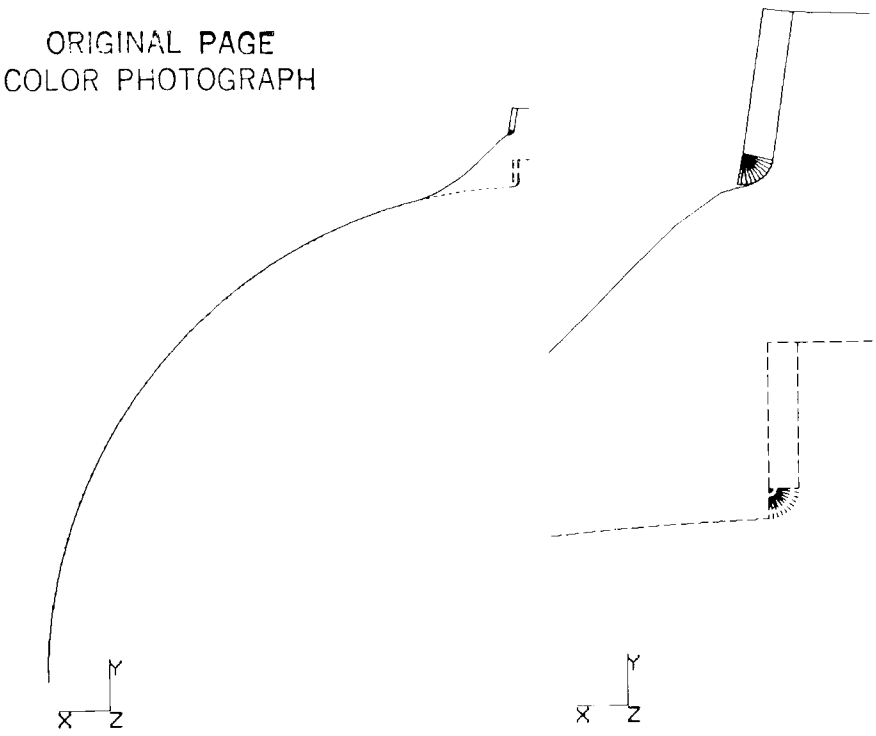


Figure 7.- Finite element model (Model 4) with refinements in the clamp bar radius - band contact region.

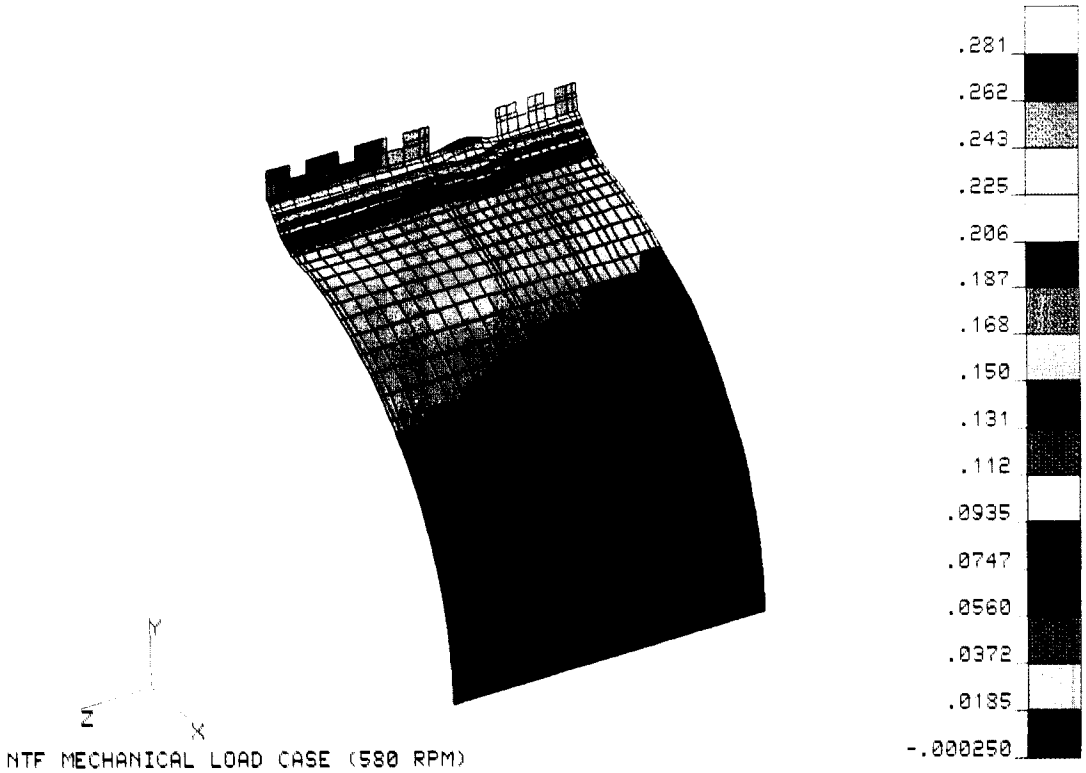


Figure 8.- Contour plot of radial deflections for the baseline centrifugal load case.

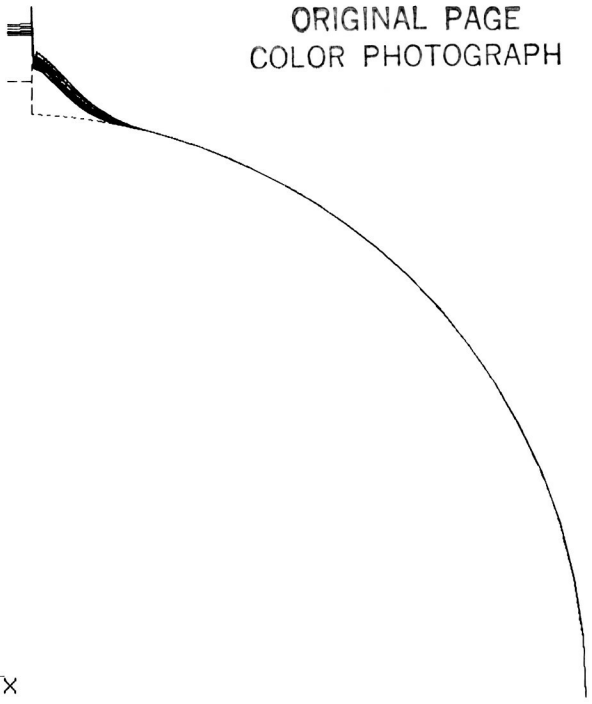


Figure 9.- Deformed geometry plot of radial deflections for the baseline centrifugal load case.

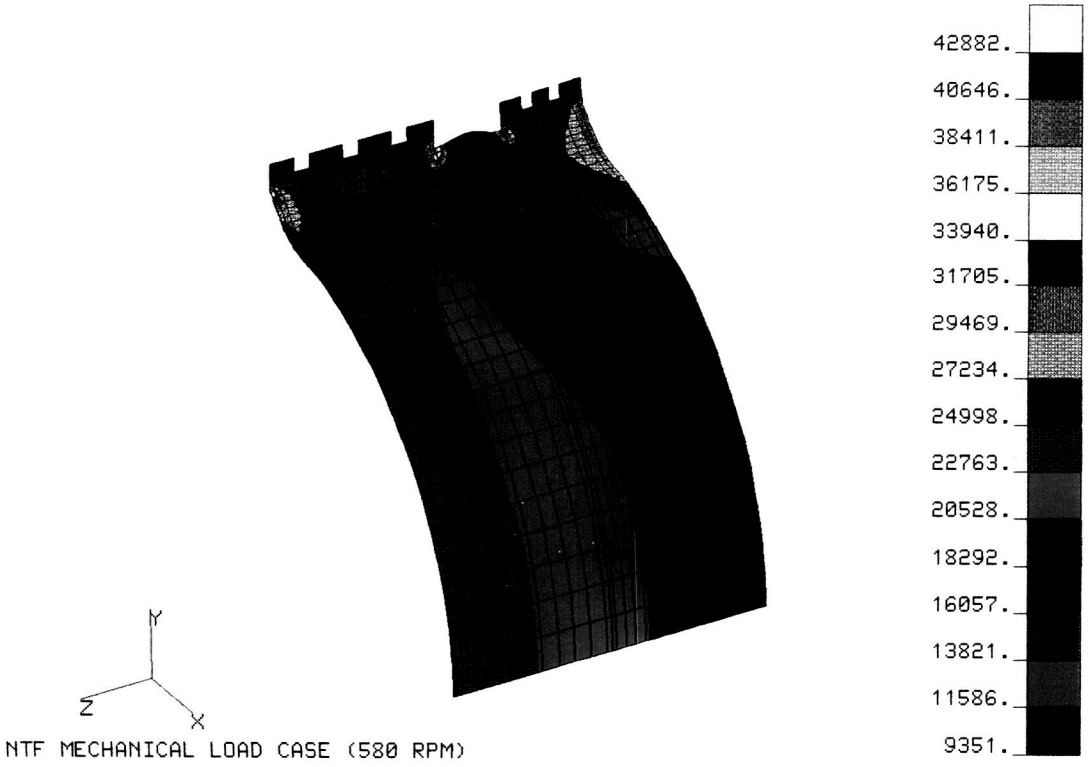


Figure 10.- Contour plot of effective stress in the band for the baseline centrifugal load case.

ORIGINAL PAGE
COLOR PHOTOGRAPH

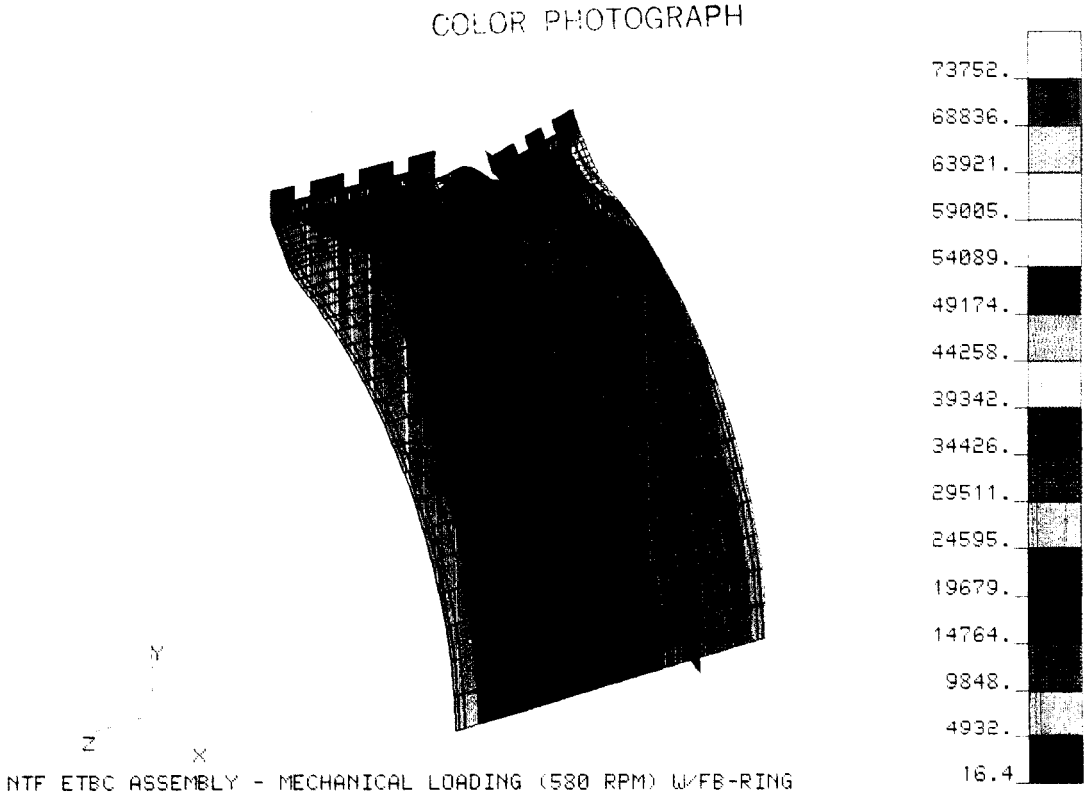


Figure 11.- Contour plot of effective stress in the band for the centrifugal load case with an unbroken ring attached.

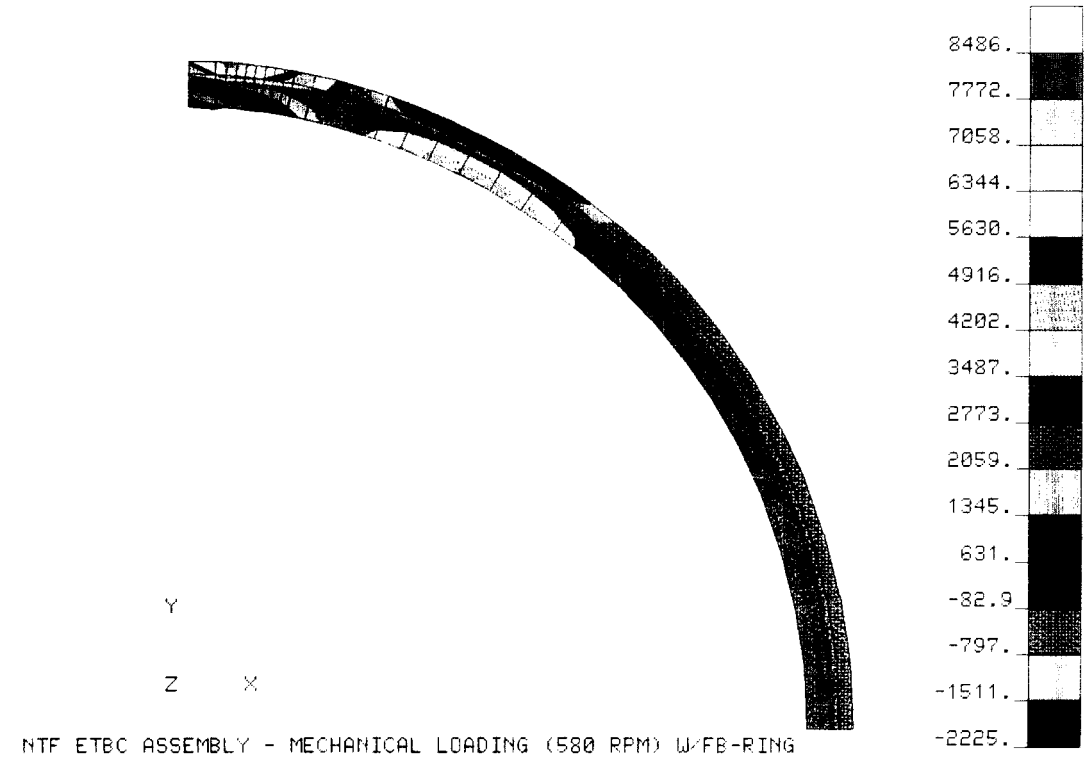


Figure 12.- Contour plot of effective stress in the ring for the centrifugal load case with an unbroken ring attached.

ORIGINAL PAGE
COLOR PHOTOGRAPH

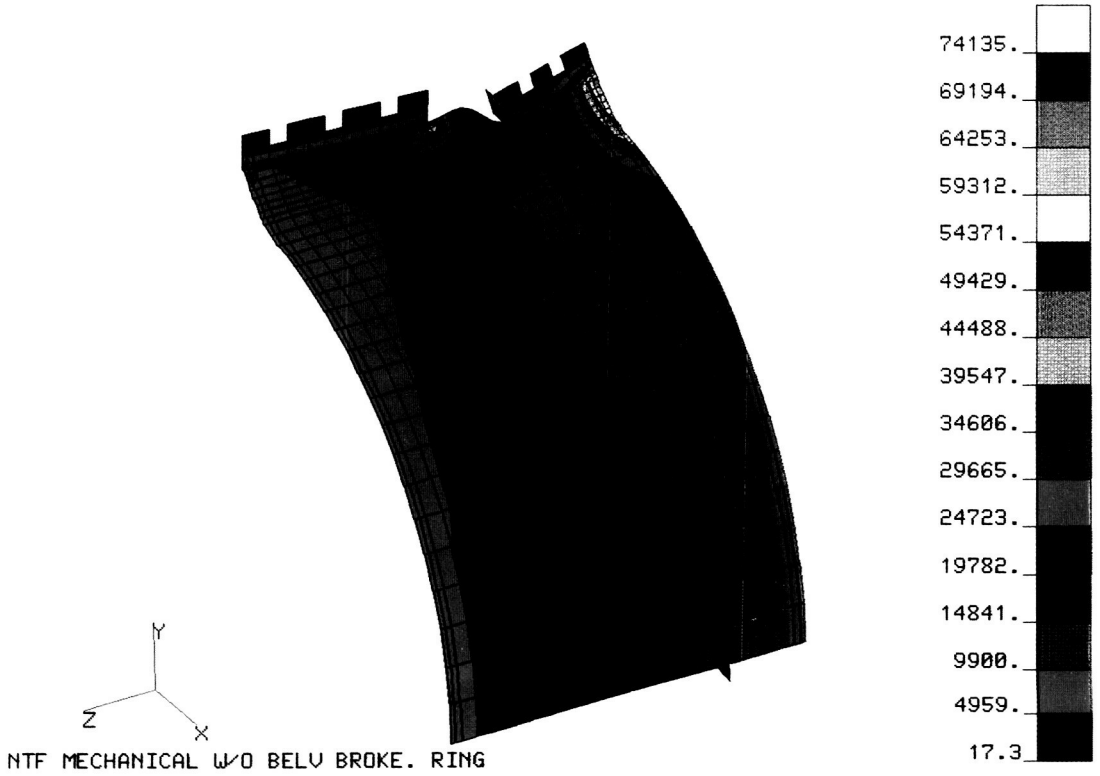


Figure 13.- Contour plot of effective stress in the band for the centrifugal load case with a broken ring attached.

ORIGINAL PAGE
COLOR PHOTOGRAPH

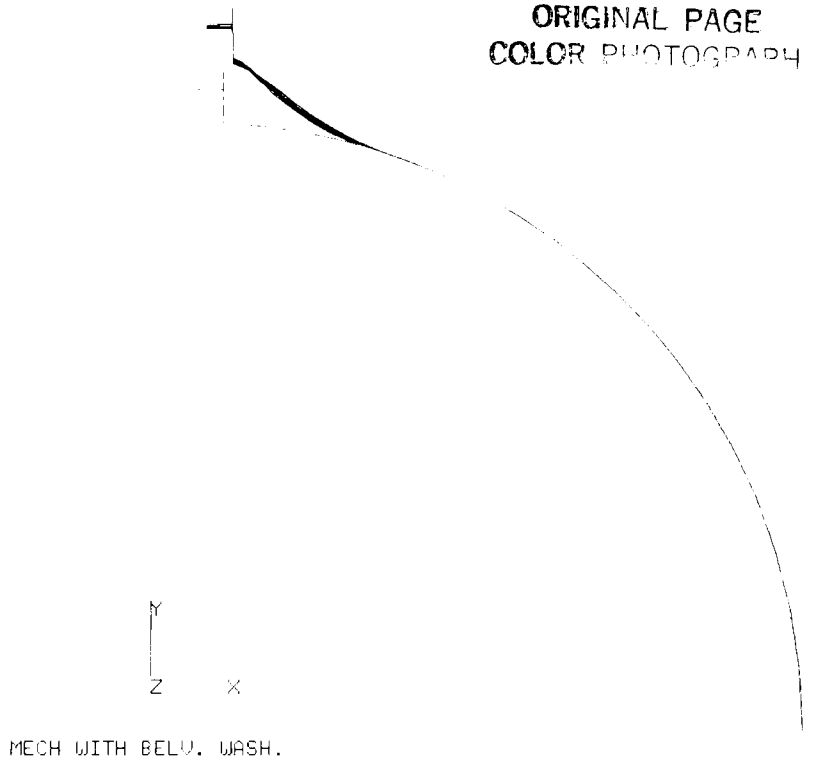


Figure 14.- Deformed geometry plot of radial deflections for the centrifugal load case with the Belleville washers effective.

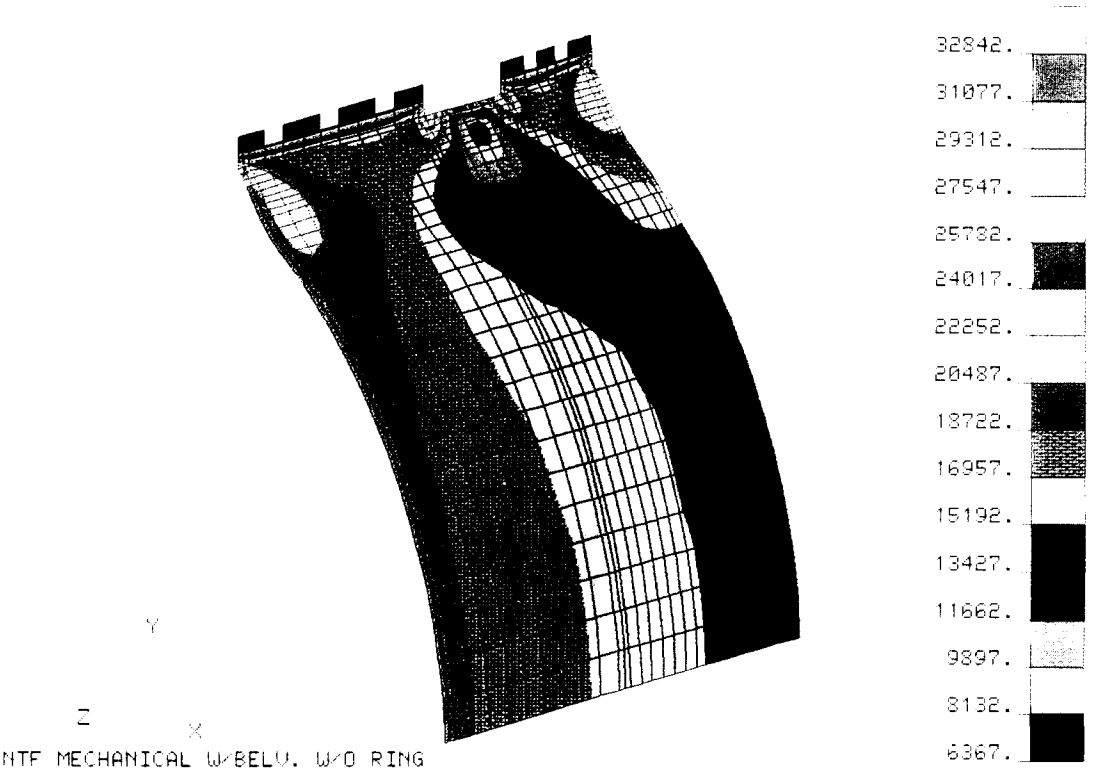


Figure 15.- Contour plot of effective stress in the band for the centrifugal load case with the Belleville washers effective.

ORIGINAL PAGE
COLOR PHOTOGRAPH

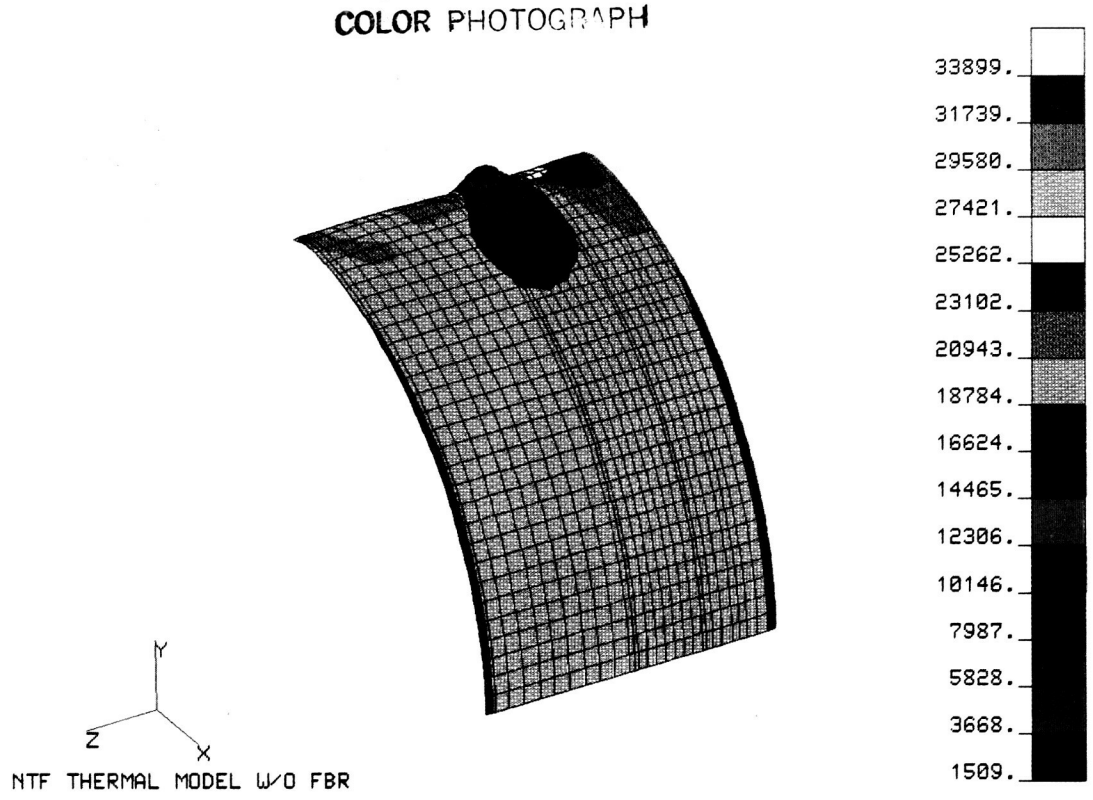


Figure 16.- Contour plot of effective stress in the band for the baseline thermal load case.

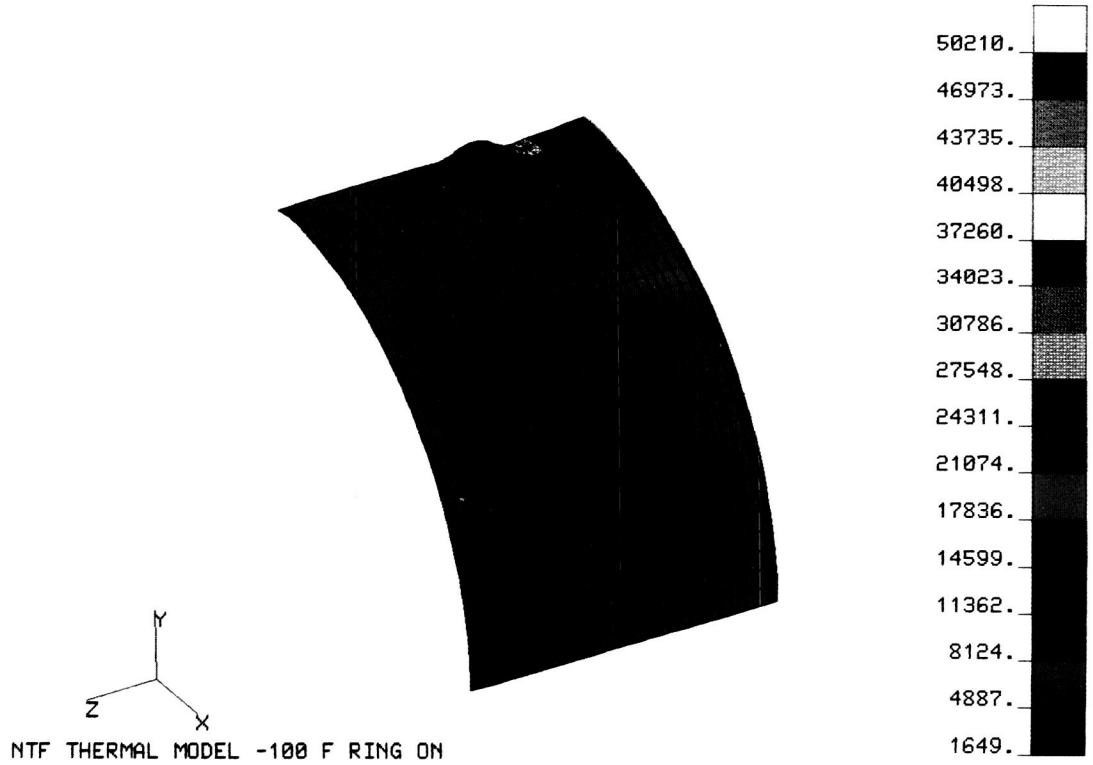


Figure 17.- Contour plot of effective stress in the band for the thermal load case with the unbroken ring attached.

ORIGINAL PAGE
COLOR PHOTOGRAPH

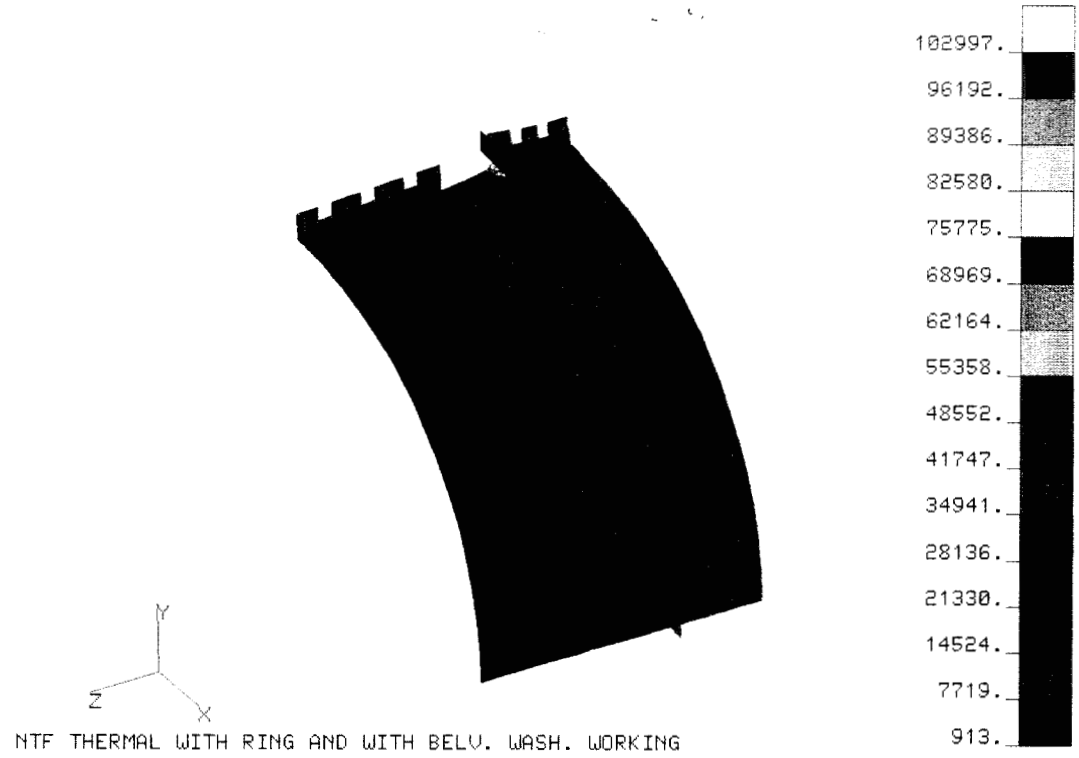


Figure 18.- Contour plot of effective stress in the band for the thermal load with the unbroken ring attached and with the Belleville washers effective.

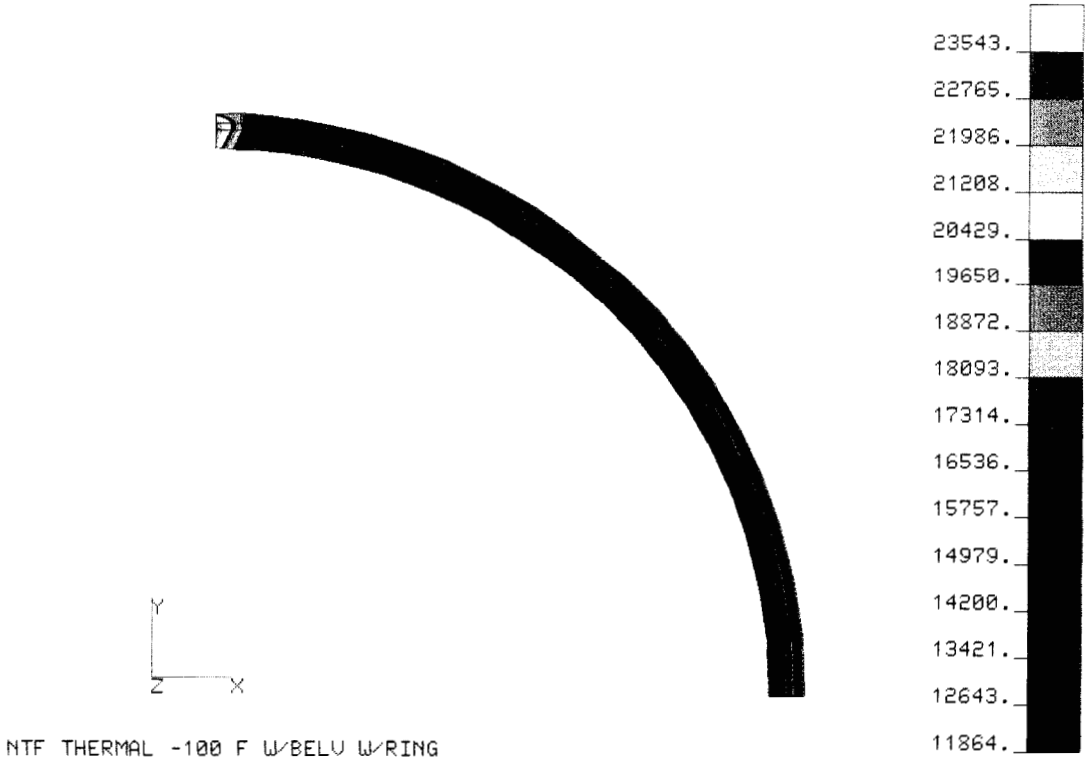


Figure 19.- Contour plot of effective stress in the ring for the thermal load with the unbroken ring attached and with the Belleville washers effective.

ORIGINAL PAGE
COLOR PHOTOGRAPH

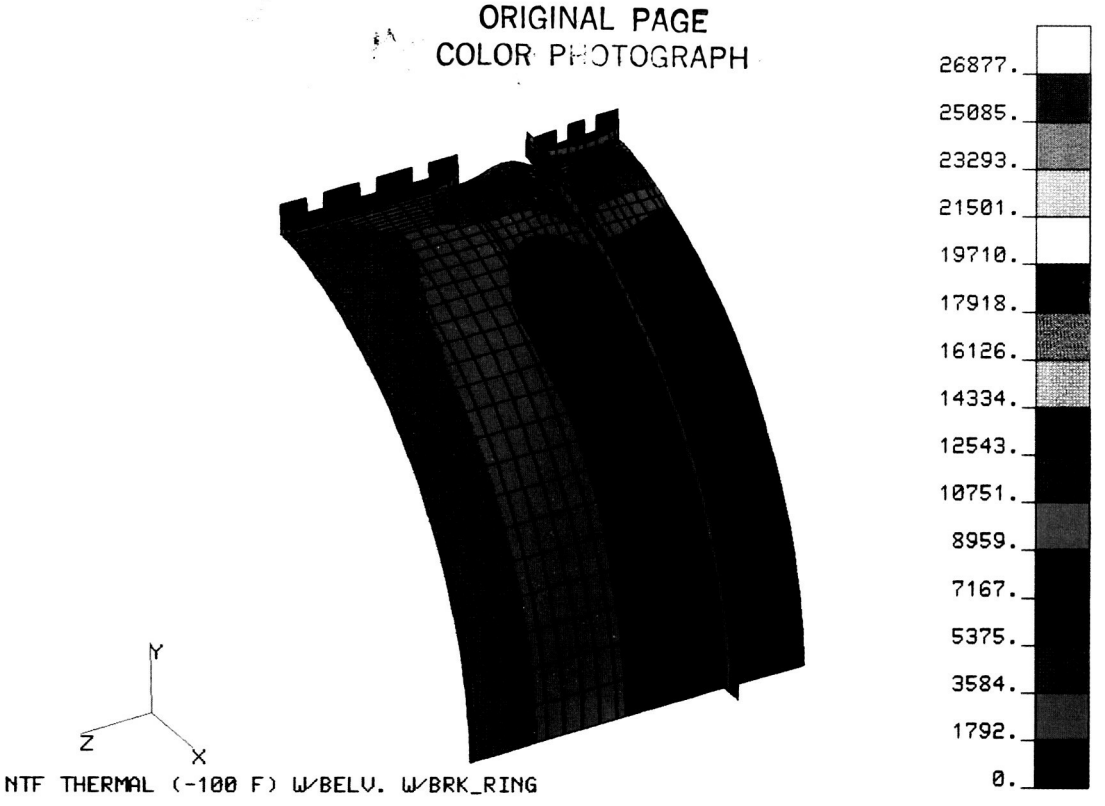


Figure 20.- Contour plot of effective stress in the band for the thermal load with the broken ring attached and with the Belleville washers effective.

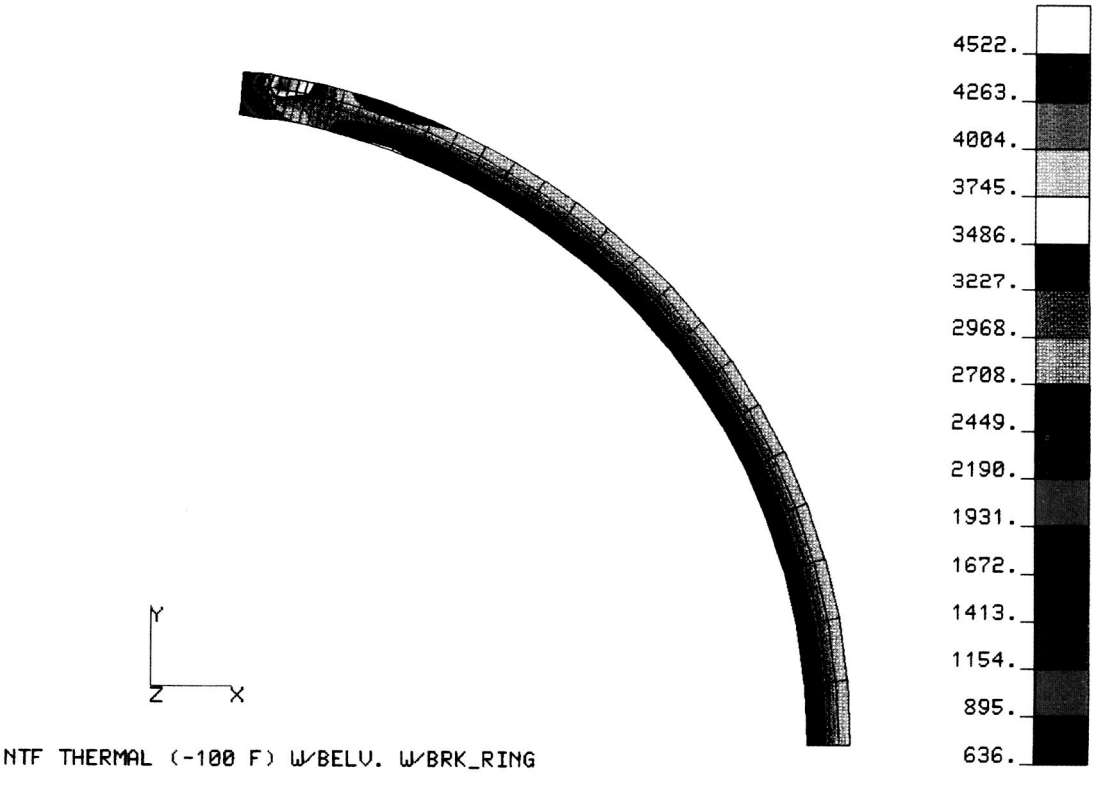


Figure 21.- Contour plot of effective stress in the ring for the thermal load with the broken ring attached and with the Belleville washers effective.

NASA
National Aeronautics and Space Administration

# Report Documentation Page

| 1. Report No. | 2. Government Accession No. | 3. Recipient's Catalog No. |
|---|---|---|
| NASA TM-101580 | | |

| 4. Title and Subtitle | 5. Report Date |
|---|---|
| Structural Analysis of a Thermal Insulation Retainer Assembly | July 1989 |
| | 6. Performing Organization Code |
| 7. Author(s) | 8. Performing Organization Report No. |
| William H. Greene and Carl E. Gray, Jr. | |
| 9. Performing Organization Name and Address | 10. Work Unit No. |
| NASA Langley Research Center<br>Hampton, VA 23665-5225 | 506-43-41-02 |
| | 11. Contract or Grant No. |
| 12. Sponsoring Agency Name and Address | 13. Type of Report and Period Covered |
| National Aeronautics and Space Administration<br>Washington, DC 20546-0001 | Technical Memorandom |
| | 14. Sponsoring Agency Code |

15. Supplementary Notes

16. Abstract

In January 1989 an accident occurred in the National Transonic Facility wind tunnel at NASA Langley Research Center that was believed to be caused by the failure of a thermal insulation retainer. This paper reports on a structural analysis of this retainer assembly in order to understand the possible failure mechanisms. Two loading conditions are important and were considered in the analysis. The first is the centrifugal force due to the fact that this retainer is located on the fan drive shaft. The second loading is a differential temperature between the retainer assembly and the underlying shaft. Geometrically nonlinear analysis is required to predict the stiffness of this component and to account for varying contact regions between various components in the assembly. High, local stresses develop in the band part of the assembly near discontinuities under both the centrifugal and thermal loadings. The presence of an aluminum ring during a portion of the part's operating life was found to increase the stresses in other regions of the band. Under the centrifugal load, high bending stresses develop near the intersection of the band with joints in the assembly. These high bending stresses are believed to be the most likely cause for failure of the assembly.

| 17. Key Words (Suggested by Authors(s)) | 18. Distribution Statement |
|---|---|
| Finite element analysis<br>Nonlinear analysis<br>Wind tunnels | Unclassified—Unlimited<br><br>Subject Category 39 |

| 19. Security Classif.(of this report) | 20. Security Classif.(of this page) | 21. No. of Pages | 22. Price |
|---|---|---|---|
| Unclassified | Unclassified | 26 | A03 |



For sale by the National Technical Information Service, Springfield, Virginia 22161-2171